Development 134, 4357-4367 (2007) doi:10.1242/dev.010678

# SCAR/WAVE and Arp2/3 are crucial for cytoskeletal remodeling at the site of myoblast fusion

**Brian E. Richardson[1,2], Karen Beckett[1], Scott J. Nowak[1] and Mary K. Baylies[1,2,*]**

Myoblast fusion is crucial for formation and repair of skeletal muscle. Here we show that active remodeling of the actin cytoskeleton is essential for fusion in *Drosophila*. Using live imaging, we have identified a dynamic F-actin accumulation (actin focus) at the site of fusion. Dissolution of the actin focus directly precedes a fusion event. Whereas several known fusion components regulate these actin foci, others target additional behaviors required for fusion. Mutations in *kette/Nap1*, an actin polymerization regulator, lead to enlarged foci that do not dissolve, consistent with the observed block in fusion. Kette is required to positively regulate SCAR/WAVE, which in turn activates the Arp2/3 complex. Mutants in *SCAR* and *Arp2/3* have a fusion block and foci phenotype, suggesting that Kette-SCAR-Arp2/3 participate in an actin polymerization event required for focus dissolution. Our data identify a new paradigm for understanding the mechanisms underlying fusion in myoblasts and other tissues.

**KEY WORDS: Cell-cell fusion, Myoblast fusion, Muscle, Actin, Kette (Hem, Nap1), SCAR (WAVE), Arp2/3**

## INTRODUCTION

Cell-cell fusion plays a crucial role in a range of processes, including fertilization, bone remodeling and muscle formation and growth, during the development of multicellular organisms (Chen and Olson, 2005). In addition, intercellular fusion has been confirmed as a primary mechanism of tissue repair used by stem cells (Alvarez-Dolado et al., 2003; Wang et al., 2003; Weimann et al., 2003). Although much is known about the molecules and mechanisms underlying intracellular fusion of membrane compartments, the molecular mechanisms underlying cell-cell fusion are not well understood. Increased knowledge of cell-cell fusion would have significant advantages for tissue engineering and repair.

During the development and repair of muscle, mononucleated myoblasts fuse to form multinucleated muscle fibers (Abmayr et al., 2003; Chen and Olson, 2004; Horsley and Pavlath, 2004; Patel et al., 2002). Fusion in *Drosophila* requires two cell types: founder cells (FCs), which seed specific muscles, and fusion-competent myoblasts (FCMs), which fuse to an FC and adopt that FC muscle program (Baylies et al., 1998; Carmena and Baylies, 2006; Frasch, 1999). As a result of fusion, a muscle of particular size, shape and orientation forms. There are 30 individual muscles per hemisegment of the *Drosophila* embryo; depending on the particular muscle, body wall muscles in *Drosophila* embryos fuse between two and 25 times (Bate, 1990).

A number of mutations have been identified in *Drosophila* that disrupt fusion (Abmayr et al., 2003; Chen and Olson, 2004; Taylor, 2003). The genes revealed by these mutations have been organized into a model based on genetics, biochemistry and predicted function. The sum of the activities of these genes lead to undefined rearrangements in the cytoskeleton that are necessary for fusion (Chen and Olson, 2004). Recognition and adhesion between an FC and FCMs are mediated by four, single-pass transmembrane proteins belonging to the immunoglobulin (IG)-domain containing family of adhesion molecules. Two are required in FCs, Dumbfounded [Duf; also known as Kirre – FlyBase (Ruiz-Gomez et al., 2000)] and Roughest [Rst; also known as Irregular Chiasm-C; IrreC (Strunkelnberg et al., 2001)], and two are required in FCMs, Sticks and stones [Sns (Bour et al., 2000)] and Hibris [Hbs (Artero et al., 2001; Dworak et al., 2001)]. Downstream of these adhesion proteins in the FC, signal transduction bifurcates, with one branch of the pathway mediated by the scaffold protein Rolling pebbles [Rols; also known as Antisocial; Ants (Chen and Olson, 2001; Menon and Chia, 2001; Rau et al., 2001)], and the second branch mediated by Loner [also known as Schizo – FlyBase (Chen et al., 2003)], a GEF (guanine nucleotide exchange factor) protein. Rols relays adhesion to components of the cytoskeleton (Menon and Chia, 2001; Zhang et al., 2000). Rols has been shown to physically interact with Duf and Myoblast city (Mbc), the *Drosophila* Dock180 homolog (Chen and Olson, 2001; Erickson et al., 1997; Rushton et al., 1995). Based on work in other systems, Mbc regulates Rac activation (Hasegawa et al., 1996; Kiyokawa et al., 1998; Nolan et al., 1998). Removal of two of the three *Drosophila* Rac homologs, Rac1 and Rac2, leads to a fusion block (Hakeda-Suzuki et al., 2002; Luo et al., 1994).

Loner, a GEF that interacts with Duf, regulates the small GTPase, ARF6 (also known as Arf51f – FlyBase) (Chen et al., 2003). ARF6 is required for cell shape changes and enhances the activity of Rac to form membrane ruffles (Donaldson, 2003; Radhakrishna et al., 1999; Zhang et al., 1999). In *loner* mutants, Rac localization is aberrant (Chen et al., 2003). Hence, Loner, through its regulation of ARF6 and Rac, leads to alterations in the cytoskeleton required for myoblast fusion.

Blown fuse (Blow), a PH-domain containing protein (Doberstein et al., 1997), and Kette (also known as Hem and Nap1) (Schroter et al., 2004), are also required for fusion. Kette functions in a conserved complex with Sra-1 (also known as Pir121 and CYFIP), Abi and HSPC300 to regulate the activity of SCAR (also known as WAVE). SCAR, in turn, activates Arp2/3-dependent actin polymerization (Ibarra et al., 2005; Machesky and Insall, 1998; Smith and Li, 2004; Vartiainen and Machesky, 2004). How the Kette complex regulates SCAR is a subject of debate, as both positive and negative interactions have been suggested (Bogdan and Klambt, 2003; Eden et al., 2002; Ibarra et al., 2006; Kunda et al., 2003; Rogers et al., 2003). Recent studies have identified mutations in *WASP* (also known as *WASp* – FlyBase) and its regulator *solitary* [*sltr*; also known as *WASP-*

[1]Program in Developmental Biology, Sloan Kettering Institute and [2]Weill Graduate School at Cornell Medical School, New York, NY 10021, USA.

*Author for correspondence (e-mail: m-baylies@ski.mskcc.org)

**Accepted 14 September 2007**

*interacting protein* (*WIP*) and *Verprolin 1* (*Vrp1*)] that disrupt myoblast fusion (Kim et al., 2007; Massarwa et al., 2007; Schafer et al., 2007). Similarly to SCAR, WASP is an activator of Arp2/3-dependent actin polymerization, underscoring the importance of this pathway in fusion. Sltr is recruited to sites of myoblast adhesion and is proposed to regulate actin polymerization at these sites in FCMs (Kim et al., 2007; Massarwa et al., 2007).

Two questions raised by the genetic analyses are: (1) what is the nature of the cytoskeletal rearrangements at the site of fusion? and (2) what are the contributions of the identified proteins to this cytoskeleton remodeling at the fusion site? Here we apply novel methods in *Drosophila* to investigate the mechanisms underlying cell-cell fusion. We find a specific actin rearrangement at the fusion site, an actin focus, whose formation and dissolution precedes a fusion event. Analysis of fusion mutants has identified separable classes of genes required for the formation and dissolution of these fusion-specific actin structures. Likewise, the recruitment of the known proteins involved in myoblast fusion is altered in certain classes of mutants. By investigating the most actin-proximal of the known fusion mutants, *kette*, we find that Kette is required for the dissolution of actin foci. Mechanistically, we determined that the abnormally large foci result from the loss of positive regulation by Kette on SCAR: *kette* mutants show defects in SCAR localization and stability in vivo. Like *kette*, *SCAR* and *Arp2/3* mutants show defects in myoblast fusion and actin foci dissolution, suggesting a model in which Kette-SCAR-Arp2/3-mediated actin polymerization leads to a reorganization of the actin focus that is required for the progression of cell-cell fusion. Taken together, these data provide new perspectives on the genetic, molecular and cellular requirements of myoblast fusion.

## MATERIALS AND METHODS

### *Drosophila* genetics

Stocks were grown under standard conditions. Stocks used were *twist promoter-GFP-actin* (a gift from H. A. Müller, University of Dundee, UK), *rP298-lacZ* (Nose et al., 1998), *twist-CD2* (Dunin-Borkowski and Brown, 1995), *apME*-GFP (this study), *apME-NLS::eGFP* (this study), *apME-NLS::dsRed* (this study), *Df(1)w67k30* [deficiency removing *duf* and *rst* (Lefevre, and Green, 1972; Ruiz-Gomez et al., 2000)], $kette^{J4\text{-}48}$ (Hummel et al., 2000), $rols^{T627}$ (Chen and Olson, 2001), $loner^{T1032}$ (Chen et al., 2003), $mbc^{C1}$ (Rushton et al., 1995), $sns^{XB3}$ (Bour et al., 2000), $blow^{1}$ (Doberstein et al., 1997), $Rac1^{J11}Rac2^{\Delta}mtl^{\Delta}$ (Hakeda-Suzuki et al., 2002), $SCAR^{\Delta 37}$ (Zallen et al., 2002), $SCAR^{k13811}$ [(Spradling et al., 1999) Berkeley *Drosophila* Genome Project], $Arp3^{EP3640}$ (Rorth, 1996), and $D\text{-}WIP^{D30}$ (Massarwa et al., 2007). Mutants were balanced and identified using *CyO P[w⁺wg^en11lacZ]*, *TM3 Sb¹ Dfd-lacZ* or TTG [TM3, twi-GAL4, UAS-2xeGFP (Halfon et al., 2002)]. Germline clones (Chou and Perrimon, 1996) were generated by heat shock of *hs-FLP; ovoD*, $FRT40A/SCAR^{k13811}$, *FRT40A* larvae. Germline clone females were mated to $SCAR^{k13811}/CyO$ at 20-22°C to create $SCAR^{k13811}$ maternal/zygotic embryos (Zallen et al., 2002).

#### Germline transformation and constructs

*apME-GFP*, *apME-NLS::eGFP* (gifts from Z. Kambris and M. Capovilla, Centre National de la Recherche Scientific, Strasbourg, France) and *apME-NLS::dsRed* (this study) DNA were constructed by cloning the *apterous* mesodermal enhancer 680 into pGreenH-Pelican, pH-Stinger and pRedH-Stinger [(Barolo et al., 2000; Barolo et al., 2004; Capovilla et al., 2001) Berkeley *Drosophila* Genome Project], which, respectively, contain cytoplasmic eGFP, eGFP and dsRed.T4 downstream of a nuclear localization signal. Constructs were injected using established protocols (Beckett and Baylies, 2006).

#### Immunohistochemistry

Embryos were collected at 25°C on apple juice agar plates and were fixed as described previously (Beckett and Baylies, 2006) except that embryos were fixed in 4% EM grade paraformaldehyde (Electron Microscopy Sciences) in 0.2 M sodium phosphate for Kette and SCAR staining. Embryos were mounted in Prolong Gold (Molecular Probes) for fluorescent stainings or Araldite otherwise. Antibodies were preabsorbed (PA) where noted and used at the indicated final dilutions: mouse anti-β-galactosidase (1:1000, Promega), chicken anti-β-galactosidase (1:1000, Cappel), rabbit anti-Lame duck (LPA, 1:250) (Duan et al., 2001), rabbit anti-Kette (1:1000) (Hummel et al., 2000), guinea pig anti-SCAR (1:500) (Zallen et al., 2002), mouse anti-GFP (1:400, Clontech), mouse anti-Rols7 (1:4000) (Menon and Chia, 2001), rat anti-Loner (PA, 1:300) (Chen et al., 2003), mouse anti-Rac1 (1:200, BD Biosciences), rat anti-Mbc (PA, 1: 100) (Erickson et al., 1997), rat anti-Sticks and stones (Sns, 1:100) (Bour et al., 2000), rabbit anti-Blow (PA, 1:500) (Doberstein et al., 1997), rabbit anti-Slouch (PA, 1:200) (Beckett and Baylies, 2007) and rabbit anti-myosin heavy chain (Mhc; 1:10000; a gift from D. Kiehart, Duke University, Durham, NC). Biotinylated secondary antibodies (Vector Laboratories and Jackson ImmunoResearch) and the Vectastain ABC kit (Vector Laboratories) were applied for non-fluorescent Mhc stainings. Additionally, TSA amplification (PerkinElmer Life Sciences) was applied for Kette, Scar, Loner, Sns and Rac1. We used Alexa Fluor 488-, Alexa Fluor 555- and Alexa Fluor 647-conjugated fluorescent secondary antibodies and Alexa Fluor 546- and Alexa Fluor 647-conjugated phalloidin (Invitrogen). Fluorescent images were acquired on a Zeiss LSM 510 confocal scanning system mounted on an Axiovert 100M microscope with a 63× 1.2 NA C-Apochromat water objective. For confocal microscopy, pinholes were set to capture an optical slice of 1.1 μm. Non-fluorescent images were acquired on a Zeiss Axiophot microscope. Images were processed using Adobe Photoshop. 3D reconstruction was created using Improvision Volocity software.

#### Live imaging

Embryos were collected and dechorionated in 50% bleach for 3 minutes. Appropriately staged embryos were selected and mounted on glass-bottom Petri dishes (MatTek Cultureware) using Technau glue (Scotch tape dissolved in heptane) and covered with halocarbon 700 oil (Halocarbon Products). GFP was excited at 488 nm and dsRed was excited at 543 nm. All pinholes were set to capture an optical slice of 1.5 μm. All timelapse sequences were taken as a series of *z*-stacks over time (4D imaging), with optical sections captured every 1.5 μm. Fusion events were only considered valid if optical slices were available above and below the plane of fusion, to rule out mistaking a cell migration event for myoblast fusion. Optical projections were created using the projection function of the Zeiss LSM software. Images were processed with Adobe Photoshop, and movies were created from image sequences using Apple Quicktime.

#### Foci size and duration measurements

Area was measured using the overlay function of the Zeiss LSM software (see Fig. S2 in the supplementary material). Foci were measured in the optical slice where they had the greatest radius and where FC-FCM adhesion was verified with specific cell labeling. The edges of foci were determined by using the range indicator function of the software and setting the edge where there is a clear change from signal to background. Measurements were acquired in the linear range of intensity and no relevant pixels were saturated. Duration was calculated as the time between when a focus appeared in a sequence and when it disappeared from detection. Foci were only included for duration measurements if there were optical slices above and below throughout the sequence to ensure actual dissolution and rule out cell/foci movement. Statistical analysis was performed with Microsoft Excel.

## RESULTS

### Actin rearrangements during the period of myoblast fusion

To define the behavior of the actin cytoskeleton during myoblast fusion [stages 12-15, 7.5-13 hours AEL (after egg laying) (Bate, 1990; Beckett and Baylies, 2007)], fixed wild-type embryos were stained with phalloidin to label filamentous actin (F-actin) and with specific reagents that distinguish FCs/myotubes and FCMs. *rp298-lacZ* expresses β-galactosidase in the nuclei of FCs (Nose et al., 1998), whereas Lame duck (Lmd) is an FCM-specific transcription

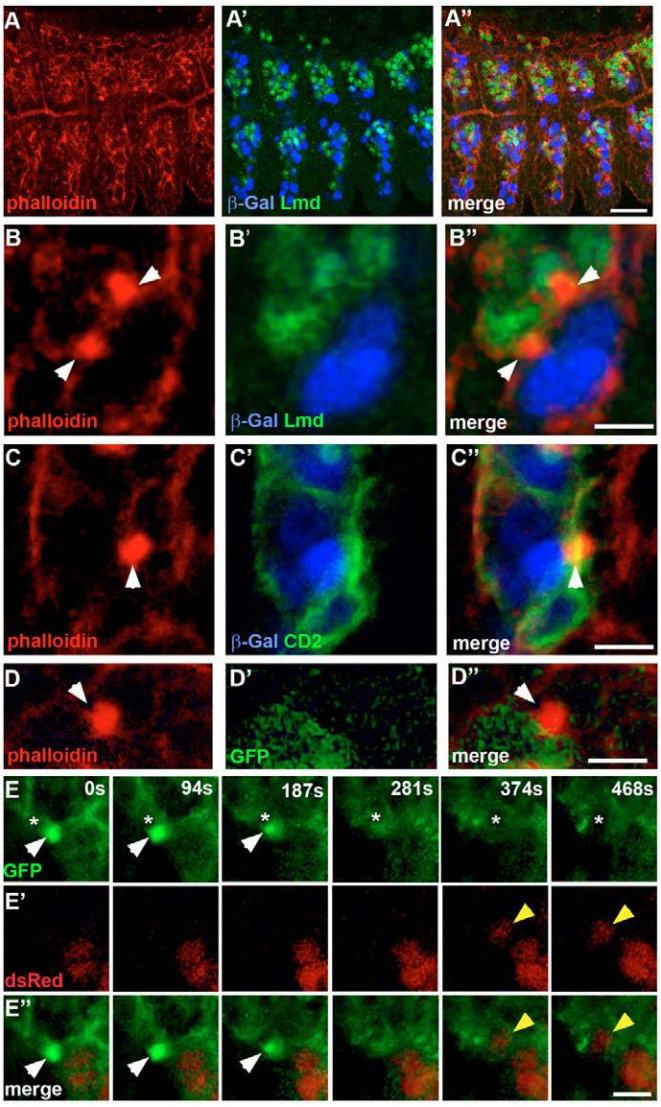


**Fig. 1. Dynamic remodeling of the actin cytoskeleton during *Drosophila* myoblast fusion.** Lateral views of stage 14 embryos. Phalloidin was used to label F-actin (red) in A-D. (**A-A″**) *rP298-lacZ* embryo stained with phalloidin and antibodies against ß-galactosidase to label FCs/myotubes (blue), and Lame duck to label FCMs (green). These images show the arrangement of myotubes and FCMs in one plane of focus and the occurrence of F-actin foci at this stage. F-actin is seen predominantly at the cell cortices. (**B-B″**) Higher magnification of A. F-actin foci form at the adhesion sites between FCs/myotubes and FCMs (arrowheads). For 3D reconstruction of an actin focus, see Movie 1 in the supplementary material. (**C-C″**) *rP298-lacZ; twi-CD2* embryo stained with phalloidin and antibodies against β-galactosidase to label FCs/myotubes (blue), and CD2 to label mesoderm cell membranes (green). An actin focus is present in both the FC and the FCM, as evident by bisection of the focus with membrane staining (arrowhead). (**D-D″**) *apME-GFP* embryo stained with phalloidin and antibody against GFP to label the cytoplasm of *apterous*-expressing FCs/myotubes (green). GFP does not leak from the *apterous*-expressing myotube into the adherent FCM when the F-actin focus is present. (**E-E″**) Live *twi-GFP-actin*, *apME-NLS-dsRed* embryo. Each column of panels represents a time point from a timelapse sequence. Each image is an optical projection displaying 9 μm of the *z*-axis. The optical projection allows visualization of several cell layers simultaneously and tracking of all relevant cell movements. In this sequence, an actin focus (white arrowheads) forms at the adhesion site between an FCM and an *apterous*-labeled myotube. This focus dissolves, followed by fusion and addition of a labeled nucleus (yellow arrowhead) to the myotube. The nucleus of the fusing cell is indicated (asterisk). Additional actin accumulation in 468-second panel may represent a new actin focus forming. Scale bars: 20 μm in A; 5 μm in B-E.

factor that has both nuclear and cytoplasmic expression (Duan et al., 2001; Nose et al., 1998) (Fig. 1A,B, and see Fig. S1A,B in the supplementary material). Hence, the relevant myoblast cell types, their arrangements with respect to one another and changes in actin cytoskeleton could be identified during fusion.

In addition to a uniform accumulation of F-actin at the myoblast cell cortex (Fig. 1A,B, and see Fig. S1A,B in the supplementary material), specific F-actin structures were observed. First, F-actin-based filopodia and lamellopodia were observed in both FCs and FCMs. FCMs extended filopodial projections directionally towards an FC/myotube (see Fig. S1A in the supplementary material). These data are consistent with the migration of FCMs from internal layers externally to fuse with myotubes (Beckett and Baylies, 2007). As recognition occurred between an FC/myotube and FCM, the FCMs assumed a tear-drop shape, and this change in cell shape was reflected in the actin cytoskeleton (see Fig. S1B in the supplementary material). At the sites of adhesion between FCs/myotubes and FCMs, we observed a striking accumulation of F-actin in foci (Fig. 1B and see Movie 1 in the supplementary material) (Kim et al., 2007; Kesper et al., 2007). These foci were most often spherical and located across both cell types (Fig. 1C). To better characterize actin foci, we measured their size (see Fig. S2 in the supplementary material). In wild-type embryos, these foci ranged in size from 0.7-4.5 $\mu m^2$, averaging 1.9 $\mu m^2$ ($n$=100 foci; Table 1). The range observed in these fixed preparations most likely reflects the dynamic nature of the actin foci (see below). Actin foci were not observed in non-mesodermal tissues nor were they detected in mesodermal cells before or after the stages when fusion takes place (see Fig. S3A,C in the supplementary material). Furthermore, actin foci are present prior to pore formation in membranes between myotubes and FCMs, as cytoplasmic GFP expressed specifically in myotubes does not leak across foci into the cytoplasm of adherent FCMs (Fig. 1D). Thus, using these labeling techniques, a series of actin cytoskeletal behaviors that occur during muscle and myotube formation have been identified: actin-rich protrusive structures, cell shape changes and an accumulation of F-actin at the adhesion site between FCs/myotubes and FCMs.

## Live imaging reveals dynamics of actin-based behaviors and the site of myoblast fusion

To reveal the dynamics of these actin-based behaviors and their contribution to the fusion process, timelapse analysis of live embryos was employed. A GFP-actin fusion protein was expressed in all myoblasts under the control of the *twist* promoter (*twi*p) (Verkhusha et al., 1999). Phalloidin staining of *twi*p-*GFP-actin* embryos confirmed that both methods revealed the same range of actin-based rearrangements described above (see Fig. S1C-E, Fig. S4 in the supplementary material). In particular, GFP-actin foci were observed at FC/myotube and FCM adhesion sites to be of similar size and shape to the phalloidin-stained F-actin foci (mean: 1.8 $\mu m^2$, range: 0.7-4.7 $\mu m^2$, $n$=25, Fig. 1E, and see Fig. S4 in the supplementary material). Live imaging revealed that an actin focus at the adhesion site builds into the spherical structure observed in fixed embryos (Fig. 1B). Actin foci are dynamic structures: the lifetime of actin foci ranged from 5.7

to 29.5 minutes with the average actin focus present for 11.9 minutes at all stages in which myoblast fusion takes place ($n$=50). Actin foci build to their maximum size in less than 2 minutes and, following their duration, completely dissolve in less than 1 minute.

We next tested whether the dynamic accumulation and dissolution of actin foci marked the site of fusion. Using our live imaging approach, we captured single fusion events of FCMs with a specific myotube (Fig. 1E and see Fig. S5, Movies 2, 3 in the supplementary material). To ensure that we were measuring myoblast fusion, we took advantage of the well established observation that, upon fusion of an FCM to a specific FC/myotube, the incorporated naïve FCM nucleus is programmed to the specific muscle identity and becomes labeled with the FC-specific identity genes, such as *slouch* or *apterous* (Baylies et al., 1998; Capovilla et al., 2001; Frasch, 1999). We therefore generated transgenic flies carrying both *twi*p-*GFP-actin*, which is expressed in all FCs and FCMs, and an *apterousME-NLS-dsRed* construct, which is expressed in a specific subset of FCs, their growing myotubes and resultant muscles. In this way, we monitored single fusion events with 4D live imaging (a 3D z-stack imaged over time) by following myoblast arrangements in time and space and by the accompanying incorporation of an additional dsRed nucleus into the *apterousME-NLS-dsRed* myotube. In all fusion events observed (>50), an ordered sequence of events takes place. First, an actin focus forms at the adhesion site between a fusing myotube, labeled with *apterousME-NLS-dsRed*, and an FCM. Next, the actin focus dissolves, followed by myoblast fusion and detection of dsRed in the newly added nucleus (≤5 minutes; Fig. 1E and see Movie 2 in the supplementary material). Identical data were obtained using *apterousME*-NLS-eGFP (see Fig. S5, Movie 3 in the supplementary material). In no case was fusion observed in the absence of actin focus formation and dissolution. Based on these studies, we concluded that the actin focus marks the site of myoblast fusion and that dissolution of the actin focus directly precedes a fusion event. In addition, these data revealed the dynamics of actin foci formation and dissolution and myoblast fusion in vivo.

## Mutations in known fusion genes affect foci differently

Since we identified a specific actin rearrangement that is directly linked to the fusion site, we next addressed whether mutations in the genes linked to myoblast fusion led to defects in actin foci number or morphology. Actin foci in mutant embryos were first examined in fixed preparations using phalloidin staining at stage 14, the period when the maximum number of fusion events takes place (Beckett and Baylies, 2007). The mutants fell into three classes based on actin foci number and size: (1) decreased number, normal size, (2) increased number, normal size, and (3) increased number, increased size (Table 1, Fig. 2 and see Fig. S2 in the supplementary material; data not shown).

Class one mutant embryos had fewer foci. Disruption of genes involved in FC-FCM recognition and adhesion, such as *duf*, *rst* and *sns* (Fig. 2B and data not shown), led to embryos with no actin foci. These data indicated that adhesion between FCs/myotubes and FCMs is critically required to initiate actin nucleation and formation of the F-actin focus. Additionally, disruption of *rols* led to a decrease in the number of actin foci, although those that did form were of normal size (Fig. 2C, Table 1 and data not shown). Antibodies to Sns and Rols colocalized with the actin foci (Fig. 3A,B), consistent with the actin foci marking the fusion site.

One mutant had increased numbers of wild-type size actin foci (class 2): *loner* (Fig. 2D; Table 1 and data not shown). The increase in the number of foci was consistent with a block in myoblast fusion in this mutant background. Despite the reported FC-specific expression of Loner (Chen et al., 2003), it was found to be consistently expressed within myotubes and FCMs, localized near foci but never overlapping (Fig. 3C and data not shown). These data, together with live imaging data (see below), suggested that, although Loner activity is required for the progression of fusion, it regulates fusion independently of actin foci.

A third class – *Rac* (*Rac1*, *Rac2*, *Mtl* triple mutants), *kette*, *blow* and *mbc* – showed enlarged foci, as well as increased numbers of actin foci (Fig. 2E-H and data not shown). Rac localization was punctate throughout the cell, with partially overlapping F-actin foci (Fig. 3D). The protein products encoded by the other genes were enriched at the sites of actin foci formation both in the myotubes and in adhering FCMs (Fig. 3E-G). Expression of these proteins in both myotubes and FCMs is consistent with published data (Erickson et

**Table 1. Actin foci size in wild type and fusion mutants**

| Genotype | Focus size (mean) | *P* value | Focus size (range) | ±s.d. |
|---|---|---|---|---|
| Wild type | 1.9 | N/A | 0.7-4.5 | 0.7 |
| *kette* | 3.4* | $5.7\times10^{-15}$ | 1.2-8.3 | 1.5 |
| *SCAR* | 2.3 | 0.014 | 1.0-6.2 | 1.1 |
| *SCAR* M/Z | 3.4* | $1.9\times10^{-8}$ | 1.0-10.8 | 2.3 |
| *Arp3* | 2.2 | 0.091 | 0.8-5.5 | 1.2 |
| *blow* | 3.7* | $1.2\times10^{-8}$ | 0.5-8.1 | 1.8 |
| *mbc* | 4.6* | $2.3\times10^{-9}$ | 1.4-10.9 | 2.5 |
| *Rac* | 3.4* | $4.7\times10^{-12}$ | 1.4-7.6 | 1.6 |
| *rols* | 2.0 | 0.57 | 0.8-5.9 | 1.0 |
| *loner* | 2.1 | 0.22 | 0.6-5.4 | 1.0 |
| *D-WIP* | 1.9 | 0.90 | 0.7-3.4 | 0.5 |

Foci were measured ($\mu m^2$) at stage 14 (see Materials and methods). Ten embryos/50 hemisegments were analyzed for wild type and *kette* mutants. Five embryos/25 hemisegments were analyzed for other mutants. Standard deviation (±s.d.) was determined for each genotype. Asterisks indicate statistical significance ($P$<0.0001) for size difference compared with wild type as determined by two-tail unpaired Student's $t$-test ($n$=100 foci for wild type and $kette^{J4\text{-}48}$; $n$=50 foci for other mutants).
N/A, not applicable.

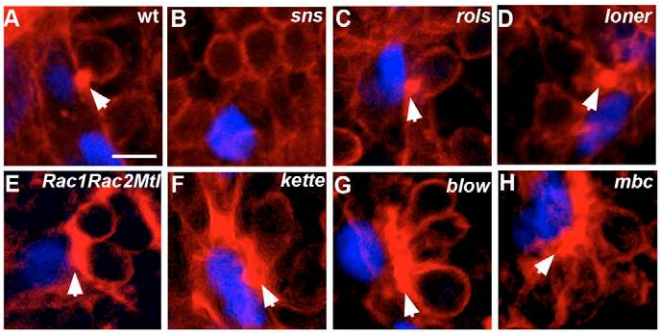


**Fig. 2. Roles of fusion proteins in actin remodeling.** Lateral views of stage 14 *rp298-lacZ* embryos stained with phalloidin to label F-actin (red) and antibody against β-galactosidase to label FCs/myotubes (blue), except E, which is stained with an antibody against Slouch to label a subset of FCs/myotubes (blue). Actin foci are indicated by arrowheads. Scale bar: 5 μm. One optical slice is shown for each mutant. For details of focus size determination, see Materials and methods and Fig. S2 in the supplementary material. (**A**) Wild type. (**B**,**C**) Class 1: no, or few foci. (B) $sns^{XB3}$ embryo. (C) $rols^{T627}$ embryo. A focus of wild-type size is occasionally seen (arrowhead). (**D**) Class 2: wild-type actin foci: $loner^{T1032}$ embryo. (**E-H**) Class 3: enlarged actin foci. (E) $Rac1^{J11}$, $Rac2^{\Delta}$, $mtl^{\Delta}$ embryo. (F) $kette^{J4\text{-}48}$ embryo. (G) $blow^{1}$ embryo. (H) $mbc^{C1}$ embryo.

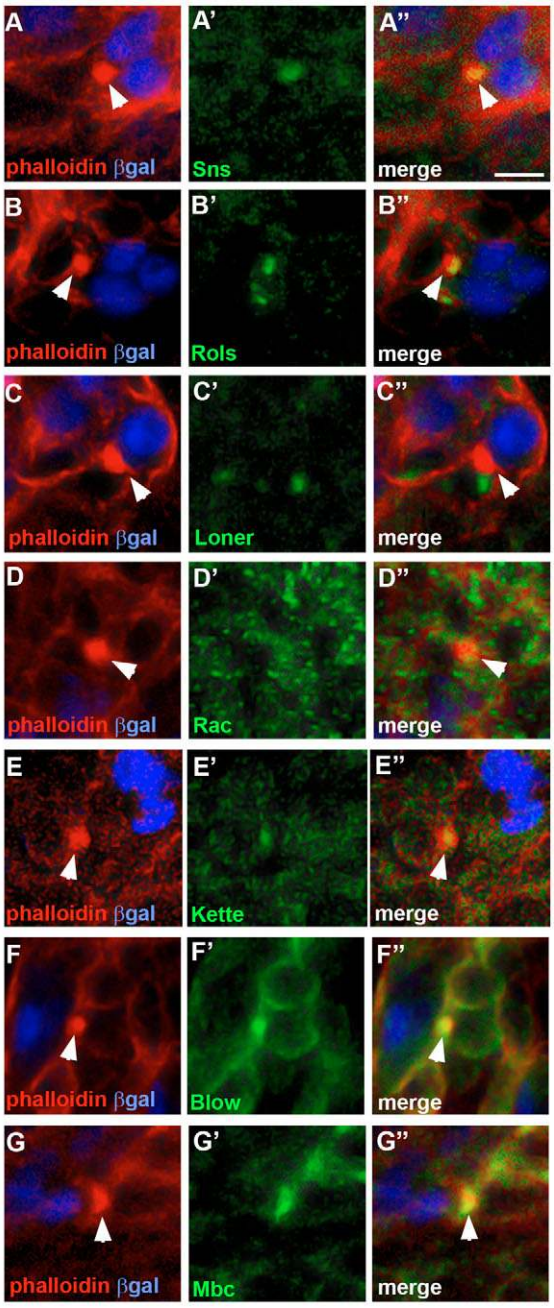


**Fig. 3. Localization of fusion machinery with actin focus.** Lateral views of stage 14 *rp298-lacZ* embryos stained with phalloidin to label F-actin (red) and antibodies against β-galactosidase to label FCs/myotubes (blue), and Sns (green, **A-A″**), Rols (green, **B-B″**), Loner (green, **C-C″**), Rac1 (green, **D-D″**), Kette (green, **E-E″**), Blow (green, **F-F″**) or Mbc (green, **G-G″**). Channels are shown separately and then merged. Sns, Rols, Kette, Blow and Mbc protein colocalize with F-actin foci (arrowheads, A,B,E,F,G), whereas Loner does not (C). Rac partially overlaps with the F-actin foci (D). Scale bar: 5 μm.

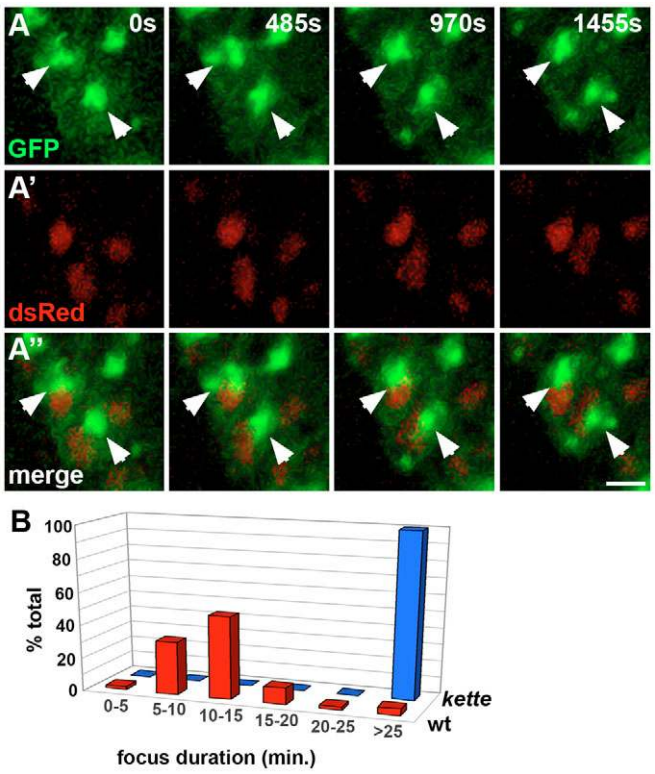


**Fig. 4. Kette regulates actin foci dissolution during *Drosophila* myoblast fusion.** (**A-A″**) Lateral views of live stage 14 *twi-GFP-actin*, *apME-NLS-dsRed*; *kette*$^{J4\text{-}48}$ embryo. Each column of panels represents a time point from a timelapse sequence. Each image is an optical projection displaying 9 μm of the *z*-axis, allowing visualization of several cell layers simultaneously and tracking of all relevant cell movements. Large actin foci form (arrowheads) but do not dissolve as in wild type (compare with Fig. 1E). No incorporation of new red nuclei is seen, consistent with the *kette* fusion block. Scale bar: 5 μm. (**B**) Actin foci persist significantly longer in *kette*$^{J4\text{-}48}$ null mutants compared to wild type. Focus duration (mean±s.d.): wild type=10.9±6.9 minutes, *kette*$^{J4\text{-}48}$=36.0±17.6 minutes. This difference is significant by a two-tail unpaired Student's *t*-test ($P$<0.0001, $n$=25 foci).

al., 1997; Schroter et al., 2006; Schroter et al., 2004). Enlarged foci were seen in these mutants from the earliest stages of fusion (data not shown), and foci persisted after fusion was complete in wild-type embryos (see Fig. S3F in the supplementary material). FCMs often clustered together at the side of adhesion to FCs in these mutants. However, distinct actin foci were often still discernable for an individual FC-FCM combination. In *kette* mutants, the average size of an actin focus was 3.4 μm$^2$, with a range of 1.2-8.3 μm$^2$ ($n$=100; Table 1). Likewise *blow*, *mbc* and *Rac* mutants had more and larger F-actin foci than wild type (Table 1, and data not shown).

Taken together, we now grouped the known fusion mutants into three distinct classes with respect to actin focus size, based on our analysis of fixed embryos. If adhesion between an FC or myotube and an FCM is impaired, no, or fewer numbers of wild-type foci were found (class 1). If there was a block in fusion after adhesion of an FCM to an FC/myotube, increased numbers of foci were found, consistent with a failure in the fusion process (classes 2 and 3). The size of the focus was, however, distinct in these two classes, with wild-type-sized foci found in class 2 mutant embryos and enlarged foci found in class 3. In addition, our finding of these two classes indicated that enlarged foci are not simply a consequence of a fusion block (see Discussion).

## Live imaging of mutants

To further understand the regulation of the actin foci at fusion sites, we performed live imaging analysis on representative mutants from the three classes of fusion mutants. Live imaging analysis of *rols*

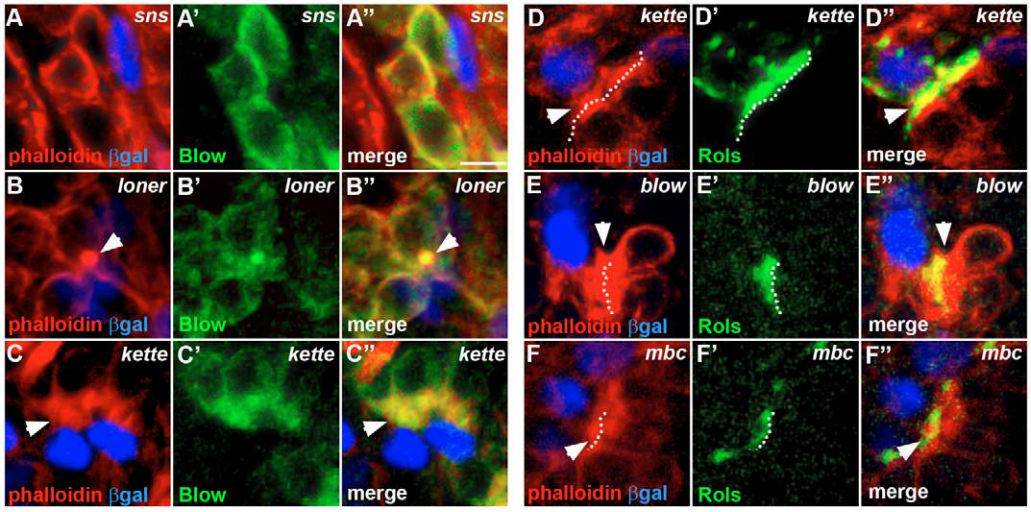


**Fig. 5. Localization of fusion machinery in different mutant classes.** Lateral views of stage 14 *rp298-lacZ* embryos stained with phalloidin to label F-actin (red) and an antibody against β-galactosidase to label FCs/myotubes (blue). Channels are shown separately and merged. Scale bar: 5 μm. (**A-C″**) Embryos stained with an antibody against Blow (green). (A) Class 1: $sns^{XB3}$ mutant. Blow no longer has a polarized localization (compare with Fig. 3F) and instead is distributed cortically in FCMs. (B) Class 2: $loner^{T1032}$ mutant. Blow localization overlaps with the actin focus (arrowhead, compare with Fig. 3F). (C) Class 3: $kette^{J4\text{-}48}$ mutant. Blow is polarized and distributed throughout large actin accumulations (arrowhead). (**D-F″**) Embryos stained with antibody against Rols to label FCs/myotubes (green). (D) $kette^{J4\text{-}48}$ mutant. (E) $blow^{1}$ mutant. (F) $mbc^{C1}$ mutant. Dotted lines indicate FC/myotube membranes and were drawn based on Rols localization. In each case, enlarged actin foci localize across both the myotube and FCM.

mutants, which are capable of some fusion, indicated that fusion always follows actin focus formation and dissolution, as in wild type (data not shown). Live imaging of *loner* mutants indicated that whereas actin foci form normally, they never dissolve, correlating with the increased numbers of foci observed and a complete fusion block (Beckett and Baylies, 2007) (data not shown). These data, taken together with the wild-type size of actin foci in *loner* mutants, suggested that the Loner-ARF6 pathway regulates fusion independently of actin foci.

Of the class of mutations that lead to the formation of abnormally large actin foci, Kette, is most directly linked to actin polymerization (Schroter et al., 2004). Kette is a member of an evolutionarily conserved complex, which regulates the activity of SCAR. SCAR, in turn, activates Arp2/3-dependent actin polymerization (Ibarra et al., 2005; Smith and Li, 2004; Vartiainen and Machesky, 2004). Live imaging of *kette* mutant embryos revealed that GFP-actin foci were larger, as seen in the fixed preparations, and persisted significantly longer than in wild-type embryos (average 36.3 minutes compared to 11.9 minutes in wild-type, $n$=25; Fig. 4A,B and see Movie 4 in the supplementary material). This measure of actin focus duration in the *kette* mutant embryos is most likely an underestimate, as actin foci were always still present at the end of an imaging sequence (see Fig. S3F in the supplementary material). Despite the changes seen in actin foci size and number in *kette* mutant embryos, the foci still formed at sites of FC/myotube-FCM adhesion. These results indicated that the fusion defect in *kette* mutant embryos (and we would suggest, in the other members of this class; data not shown) is correlated with a failure in the dissolution of actin foci at sites of fusion.

## Localization of fusion proteins in the different foci classes

We next examined the localization of members of the known fusion proteins in the three classes of fusion mutants (Fig. 5). In fusion mutants that have no actin foci (i.e. *sns*), the fusion proteins that normally localize to the myoblast fusion site lost their polarized localization. Instead, Blow and Mbc became cortically distributed, while Kette was punctate in the cytoplasm (Fig. 5A and data not shown). This suggested that adhesion is required for proper localization of this subset of fusion proteins that co-localize with the actin foci. In fusion mutants with normally sized actin foci (*loner*), the localization of this subset of fusion proteins is indistinguishable from wild-type (Fig. 5B and data not shown). Finally, in fusion mutants with enlarged actin foci (*kette*, *mbc*, *blow*, *Rac*), this subset of the known fusion proteins continued to colocalize with F-actin and were present at high levels throughout the abnormally large actin foci at sites of myoblast adhesion (Fig. 5C and data not shown). Taken together, these data indicated that the formation of an actin focus correlates with the proper localization of a specific subset of the known fusion proteins. Enlarged actin foci were associated with an accumulation of this subset of known fusion proteins that normally localize at the site of myoblast fusion. Interestingly, the localization of Loner, which does not colocalize with actin foci in wild-type embryos, was not altered in any class of mutants at the time of foci formation (data not shown).

Sltr (D-WIP) is reported to regulate the formation of actin foci specifically in FCMs (Kim et al., 2007). Therefore, we tested if foci were asymmetrically disrupted in fusion mutants with enlarged actin foci. Use of an antibody against the FC/myotube-specific protein Rols indicated that the enlarged actin foci localize across both cell types in *mbc*, *blow* and *kette* mutant embryos (Fig. 5D-F). These data suggested that, unlike Sltr (D-WIP), these gene products are not required specifically in one cell type.

## SCAR loss of function leads to a fusion block and prevents actin focus dissolution

To further understand the mechanism underlying the foci dissolution defect in *kette* mutants, we examined the function of SCAR in myoblast fusion. The regulation of SCAR by Kette has been studied in a variety of systems. Depending on the context, the

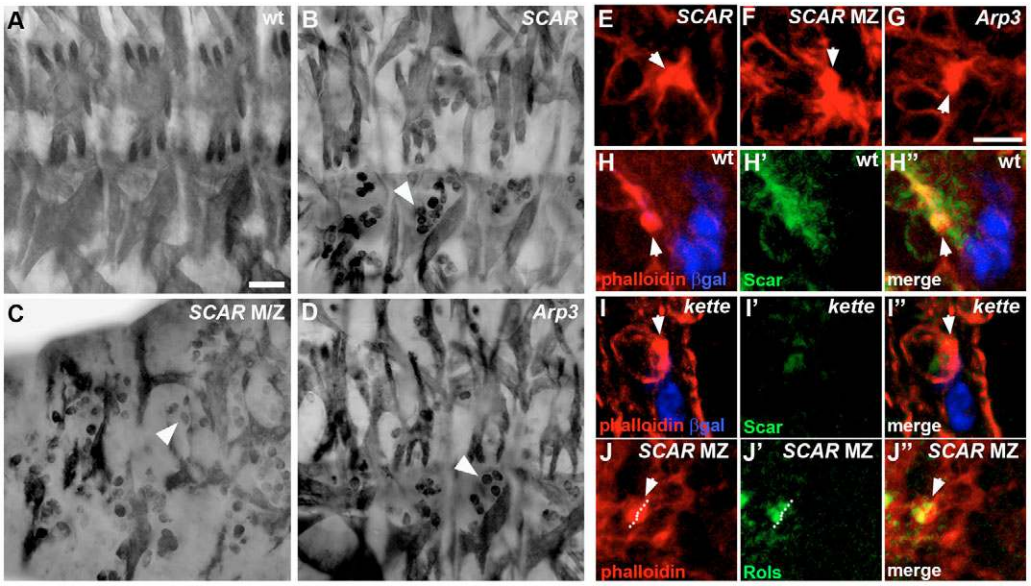


**Fig. 6. SCAR and Arp2/3 are required for myoblast fusion and regulate actin foci dissolution during fusion.** (**A-D**) Lateral views of stage 16 embryos stained with antibody against myosin heavy chain to visualize body wall muscles. Scale bar: 20 μm. (A) Wild-type embryo. (B) *SCAR*$^{\Delta 37}$ embryo. Approximately 10-20 free myoblasts (arrowhead) are seen in each hemisegment indicating a myoblast fusion defect. (C) Embryo from *SCAR*$^{k13211}$ germline clones with reduced levels of maternal and zygotic SCAR protein. Increased numbers of free myoblasts (arrowhead) are seen, along with thinner muscles, indicating a more severe myoblast fusion defect. (D) *Arp3*$^{EP3640}$ embryo. These embryos display a myoblast fusion defect, with approximately 10-20 free myoblasts (arrowhead) seen in each hemisegment. (E-J) Lateral views of stage 14 embryos stained with phalloidin to label F-actin (red). F-actin labels the foci as well as cortical actin. Scale bar: 5 μm. (**E**) *SCAR*$^{\Delta 37}$ embryo. Actin foci (arrowhead) appear larger than in wild type. The focus shown is an example of the larger foci seen in these mutants, although the average focus size is similar to wild type (Table 1). (**F**) *SCAR*$^{k13211}$ germline clone embryo with reduced levels of maternal and zygotic SCAR protein. Large accumulations of F-actin have formed at the site of adhesion between FC/myotubes and FCMs (arrowhead). (**G**) *Arp3*$^{EP3640}$ embryo. Actin foci appear larger than in wild type (arrowhead). The focus shown is an example of the larger foci seen in these mutants, although the average focus size is similar to wild type (Table 1). (**H-I″**) Embryos stained with antibodies against β-galactosidase to label FCs/myotubes (blue) and SCAR (green). (H) *rP298-lacZ* embryo. SCAR protein partially colocalizes with F-actin foci (arrowhead) in both FCMs and FCs/myotubes. (I) *rP298-lacZ*; *kette*$^{J4\text{-}48}$ embryo. SCAR protein is virtually undetectable in this mutant background. Residual protein is mislocalized (compare with H). (**J-J″**) *SCAR*$^{k13211}$ germline clone embryo stained against Rols (green). Dotted line indicates FC/myotube membrane and was drawn based on Rols localization. Rols partially overlaps with actin focus (arrowhead), indicating that enlarged actin foci localize across both FCs/myotubes and FCMs.

Kette complex is thought to negatively or positively regulate the activity of SCAR (Bogdan and Klambt, 2003; Eden et al., 2002; Ibarra et al., 2006; Kunda et al., 2003; Rogers et al., 2003). Therefore, we examined the final pattern of the embryonic musculature in *SCAR* loss-of-function mutants. Embryos homozygous for a null mutation of *SCAR* exhibited a moderate, but completely penetrant, myoblast fusion defect (Fig. 6B). Embryos with reduced maternal and zygotic *SCAR* contributions, however, had a more severe myoblast fusion defect than removal of zygotic *SCAR* alone, with increased numbers of free myoblasts and thinner muscles (Fig. 6C). Krüppel-expressing myotubes were most often mononucleate in maternal and zygotic *SCAR* mutants, with an occasional binucleate cell, suggesting a severe fusion block [1.24±0.43 nuclei/myotube (mean±s.d.) $n$=22 hemisegments; data not shown]. Altogether, these data indicated that SCAR is crucial for myoblast fusion.

We next examined actin foci in *SCAR* mutants. Analysis of F-actin foci in zygotic *SCAR* mutants revealed a range in foci size from wild-type to enlarged, with an average size being 2.3 μm$^2$ (Fig. 6E, Table 1). *SCAR* maternal and zygotic mutants showed a dramatic increase in the size and number of actin foci, to a similar level as found in *kette* mutant embryos. The average size of a mutant focus was 3.4 μm$^2$ (Fig. 6F, Table 1). Similar to Kette, SCAR expression overlapped with actin foci during myoblast fusion (Fig. 6H). However, SCAR protein levels were virtually undetectable in *kette* mutant embryos, and the residual SCAR protein was not properly localized to actin foci (Fig. 6I). These results suggested that, in the context of myoblast fusion, Kette functions as a positive regulator of the localization and stability of SCAR. In addition, the enlarged, persistent actin foci phenotypes in *kette* and *SCAR* mutants suggested that this pathway is essential, not for the formation of the actin focus, but for a crucial reorganization required for its dissolution. Moreover, the use of Rols as a marker of FCs/myotubes indicated that the enlarged actin foci localize across both cell types in *SCAR* mutants, similar to other mutants with enlarged foci (Fig. 6J).

## Arp2/3 is required for fusion

The requirement of SCAR for proper myoblast fusion and actin focus dissolution prompted us to examine the role of the Arp2/3 complex in these processes. Examination of a zygotic loss-of-function allele of Arp3/Arp66B, an essential component of the Arp2/3 complex, revealed a moderate myoblast fusion defect, similar to the defect seen in a *SCAR* zygotic loss-of-function (Fig. 6D). Likewise foci size was similar to that observed in *SCAR* zygotic mutants (Fig. 6G, Table 1). As with SCAR, this relatively mild defect could be due to the presence of maternally contributed Arp3. However, further analysis of the Arp2/3 complex is complicated by an earlier requirement, as germline clones with available reagents do not develop to the stages of muscle formation (Zallen et al., 2002). Nevertheless these data suggested that Arp2/3, like Kette and Scar, is required for actin focus dissolution.

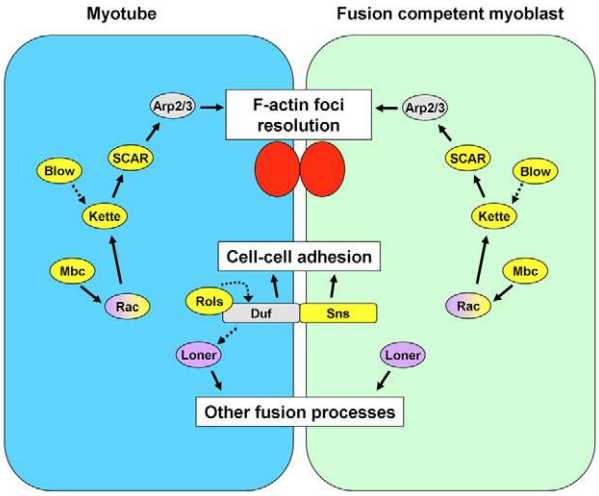


**Fig. 7. Model of *Drosophila* myoblast fusion.** Updated model of myoblast fusion based on the known fusion genes following this work. Those proteins that colocalize with the F-actin foci are colored yellow, those that do not are purple. The localization of Rac partially overlaps with actin foci. Solid arrows between proteins indicate well-established biochemical interactions, while dashed arrows indicate genetic and/or suggested, but unsubstantiated, biochemical interactions. See Discussion for details.

## DISCUSSION

Genetic analysis of the *Drosophila* muscle system has been instrumental in identifying genes that are required for one type of cell-cell fusion, myoblast fusion (Chen and Olson, 2004). Although a number of these genes have been implicated in cytoskeletal rearrangements, neither the nature of these rearrangements nor contributions of the individual genes to these rearrangements were known. We have applied novel imaging methods in *Drosophila* to investigate the cellular and molecular mechanisms underlying cell-cell fusion. Critical to a mechanistic understanding of myoblast fusion is the identification of the specific site of fusion. We have identified that site, and find that the formation and subsequent dissolution of an F-actin focus at that site directly precedes a fusion event. Our live-imaging approaches have also revealed both the dynamics of these foci and timing of cell-cell fusion, indicating that *Drosophila* myoblast fusion is a rapid process. With these new assays, we reassessed the functions of the known fusion genes, added new genes and provided a new framework for understanding the identity and sequence of cellular events required for myoblast fusion.

### Insight to cellular models of fusion

Transmission electron microscopy (TEM) analysis (Doberstein et al., 1997) has suggested that there are distinct events in the fusion process: after recognition and adhesion, the membranes between an FC and an FCM align, paired vesicles carrying electron dense material are then recruited to these sites (termed the 'prefusion complex'), these vesicles then release the electron dense material, leading to plaque formation. Subsequently, the plasma membrane breaks down, leading to cytoplasmic continuity between the cells. TEM studies indicated that, in *kette* mutant embryos, myoblast fusion is blocked at plaque formation (Schroter et al., 2004). Similarly our data indicate that in *kette* mutant embryos, fusion is blocked due to enlarged actin foci at sites of fusion. It is thus tempting to equate the actin foci with the enlarged plaques seen by TEM. However, there is a strong argument against this conclusion. We see enlarged actin foci in a number of fusion mutants, including *mbc* and *blow*. Whereas all show enlarged foci, TEM analysis reveals that only *kette* mutant embryos show a block at plaque formation. *mbc* mutant embryos show a block prior to the recruitment of the electron dense vesicles, whereas embryos mutant for *blow* show a block at the prefusion complex, with no plaque formation detected (Doberstein et al., 1997). Hence actin foci cannot be equated with the electron dense plaques.

It is consistent, however, with both data sets that the subcellular events observed by TEM, namely membrane alignment, formation of the prefusion complex and plaque formation, happen concurrently with the actin focus formation that we report here. We see that the aligned membranes are still intact when a focus is detected (Fig. 1). Recent TEM work suggests that actin is important for the targeting of vesicles (Kim et al., 2007). How the diffuse actin observed in these studies relates to the dynamic but concentrated accumulation of F-actin into foci at the plasma membrane in our study remains in question. Lastly, these observations highlight the larger question of how the events we detected with confocal microscopy relate to the events distinguished by TEM.

### Kette positively regulates SCAR-Arp2/3 to allow focus dissolution

Important to the interpretation of the mechanisms contributing to enlarged foci is our finding that SCAR and Arp2/3 are also required for myoblast fusion. Reduction of maternal and zygotic contributions of SCAR leads to a block in myoblast fusion, like that seen in *kette* mutant embryos. Reduction of zygotic Arp3 also leads to a block in fusion, although analysis of complete loss of Arp2/3 activity is precluded by the reagents currently available. Together these proteins provide an important direct link to an actin polymerization event at the site of fusion.

There has been some controversy as to how the Kette complex regulates SCAR. In biochemical assays, the Kette complex negatively regulates SCAR, holding it in an inactive state until the complex is activated by Rac (Eden et al., 2002). In support of this view, reducing the dose of *SCAR* can partially rescue the *kette* phenotype in the central nervous system of the *Drosophila* embryo (Bogdan and Klambt, 2003). By contrast, the Kette complex in *Drosophila* tissue culture cells positively regulates SCAR by correctly localizing and stabilizing SCAR (Kunda et al., 2003; Rogers et al., 2003). Our data support a positive regulation of SCAR by the Kette complex in the context of myoblast fusion. In *kette* mutant embryos, SCAR protein levels are reduced significantly and the residual protein is not localized properly. It has been suggested that the differences in SCAR regulation by the Kette complex may be a reflection of the relative differences in the amounts of SCAR and the components of the regulatory complex in different contexts (Kunda et al., 2003).

The actin focus phenotype in *SCAR* and *Arp3* mutants has also provided mechanistic insight into the role of the Kette-SCAR-Arp2/3 pathway controlling its behavior. If SCAR or Arp2/3 was required for the polymerization of actin leading to foci formation, we would have expected smaller or absent actin foci in *SCAR* and *Arp3* mutants. Instead, we find that, similar to *kette* mutants, enlarged foci are present in *SCAR* and *Arp3* mutants. These data suggest that an enlarged actin focus results from the loss of a Kette-SCAR-Arp2/3-dependent actin polymerization event required for actin foci dissolution. This actin polymerization event is presumably transient, as we have not been able to detect a site of post-focus actin

polymerization, other than cortical actin in our imaging assays. Aberrant actin accumulation in the absence of Kette and SCAR has been seen both in *Drosophila* (Hummel et al., 2000; Kunda et al., 2003; Zallen et al., 2002) and in *Dictyostelium* (Ibarra et al., 2006). These observations suggest that the Arp2/3-dependent actin polymerization machinery can function more generally in the regulation of actin cytoskeletal organization and is capable of both forming and dissolving visible F-actin structures. An additional activator of Arp2/3, WASP, may also have a potential role in the regulation of actin foci. Recent studies have indicated that WASP plays an essential role in myoblast fusion, although the regulation of actin foci was not tested (Massarwa et al., 2007; Schafer et al., 2007). Analysis of mutants in the WASP regulator, Sltr (D-WIP), indicates that actin foci do form (Kim et al., 2007). We find that the actin foci are approximately wild-type size in these mutants (Table 1).

## A revised molecular model of cell fusion

On a molecular level, the current model placed the intracellular signaling events downstream of recognition into two distinct pathways that converge on cytoskeletal rearrangements required for fusion. Our data distinguish among the identified fusion genes with respect to actin reorganization at the site of fusion. Moreover, our data suggests new relationships between the fusion mutants, leading to a revision of the existing model (Fig. 7).

Downstream of recognition and adhesion, actin foci form in the myotube and FCM. Mbc-Rac activities and the Blow-Kette-SCAR-Arp2/3 pathway acts to promote FCM cell shape change and target actin reorganization, leading to the dissolution of the actin focus in both FCMs and myotubes. Moreover, Blow and Kette have similar protein localization and actin focus phenotype, consistent with observed genetic interactions (Schroter et al., 2004). Interestingly, absence of any one of these gene products does not prohibit localization of the other members of this genetic pathway at the fusion site. Rac has been found to regulate the Kette complex in several contexts (Eden et al., 2002; Steffen et al., 2004), adding further support to this aspect of our model. Based on previous studies in a number of systems (Ibarra et al., 2005; Machesky and Insall, 1998; Vartiainen and Machesky, 2004), the target of SCAR activity is the Arp2/3 complex. Our data support this view: mutants in both *SCAR* and *Arp3* show fusion defects. Although we do not yet know how all the biochemical activities of these proteins are coordinated, the sum of the activities of all these proteins is to dissolve the actin focus, through actin reorganization in both the FCM and myotube. Our data suggests that dissolution of the focus is required for fusion to proceed and would be coupled to membrane breakdown and cytoplasmic mixing between the two cells.

A second pathway involving Loner and ARF6 also contributes to myoblast fusion. However, this pathway does not appear to directly regulate actin foci, despite the block in myoblast fusion. Unlike mutants in the Mbc-Rac-Kette-SCAR-Arp2/3 pathway, where actin focus size is dramatically increased, foci size remains wild-type in *loner* mutants. Our protein localization studies are consistent with the actin foci data: Loner does not colocalize with the actin foci, but is most often found near actin foci. Likewise, analysis of the subset of known fusion components that colocalize with the foci do not change in *loner* mutants. We predict that this pathway is required for additional behaviors, either upstream or downstream of the foci, necessary for fusion, such as myoblast searching or migration, microtubule rearrangements or other subcellular functions such as membrane trafficking.

Our data provide new insight concerning the function of Rols in myoblast fusion. Rols is proposed to serve as an adapter (Chen and Olson, 2001; Chen and Olson, 2004) between the recognition and adhesion protein Duf and Mbc, a GEF for Rac (Hasegawa et al., 1996; Kiyokawa et al., 1998; Nolan et al., 1998), linking adhesion to cytoskeletal rearrangements. Biochemical data from overexpression studies in *Drosophila* S2 cells suggest a direct interaction between Rols and Mbc (Chen and Olson, 2001). Our data, however, would indicate that this relationship is not required for focus formation and dissolution. Rols appears not to be necessary for the recruitment of Mbc to the fusion site, as average focus size is wild-type in *rols* mutants whereas it is enlarged in *mbc* mutants. Moreover, we find that localization of Rols and Mbc is not identical at foci (data not shown). Our data supports the alternative model in which Rols is required for efficient Duf recruitment to the FC membrane (Menon et al., 2005). The drastically reduced number of actin foci in *rols* mutants suggests difficulties in myoblast recognition and/or adhesion. Those actin foci that do appear are of wild-type size and correlate with fusion events, consistent with a model of reduced efficiency of fusion in *rols* mutants.

Our model leaves the function of the actin focus unresolved. Actin rearrangements can be linked to the active organization of membrane domains (Liu and Fletcher, 2006), membrane and protein trafficking (Egea et al., 2006; Kaksonen et al., 2006; Qualmann and Kessels, 2002; Stamnes, 2002), and structural support. Our data indicate that formation and dissolution of actin foci are essential for the progression of fusion. We have never observed a fusion event that has not been linked to an actin focus. The identification of the site of fusion, a particular actin structure at this site, new methods of analysis and key regulators of this structure open avenues of study for the process of cell-cell fusion in invertebrate and vertebrate biology.

We thank K. Anderson, E. Lacy, J. Zallen, A. Martinez-Arias and A. K. Hadjantonakis for discussions and critical reading of the manuscript. We also thank A. K. Hadjantonakis for imaging advice, D. Soffar for technical support, A. Muller. E. Chen, E. Schejter, D. Menon, W. Chia, S. Abmayr, R. Renkawitz-Pohl, H. Ngyugen, C. Klambt, T. Stradel, L. Cooley, J. Zallen, Z. Kambris, M. Capovilla and the Developmental Hybridoma Bank for reagents. This work was supported by Sloan Kettering Institute, NIH grants (GM 586989/GM 78318) to M.B. and a MDA Research Development Grant to S.N. (MDA4153).

### Supplementary material

Supplementary material for this article is available at
http://dev.biologists.org/cgi/content/full/134/24/4357/DC1

### References

**Abmayr, S. M., Balagopalan, L., Galletta, B. J. and Hong, S. J.** (2003). Cell and molecular biology of myoblast fusion. *Int. Rev. Cytol.* **225**, 33-89.

**Alvarez-Dolado, M., Pardal, R., Garcia-Verdugo, J. M., Fike, J. R., Lee, H. O., Pfeffer, K., Lois, C., Morrison, S. J. and Alvarez-Buylla, A.** (2003). Fusion of bone-marrow-derived cells with Purkinje neurons, cardiomyocytes and hepatocytes. *Nature* **425**, 968-973.

**Artero, R. D., Castanon, I. and Baylies, M. K.** (2001). The immunoglobulin-like protein Hibris functions as a dose-dependent regulator of myoblast fusion and is differentially controlled by Ras and Notch signaling. *Development* **128**, 4251-4264.

**Barolo, S., Carver, L. A. and Posakony, J. W.** (2000). GFP and beta-galactosidase transformation vectors for promoter/enhancer analysis in Drosophila. *Biotechniques* **29**, 726, 728, 730, 732.

**Barolo, S., Castro, B. and Posakony, J. W.** (2004). New Drosophila transgenic reporters: insulated P-element vectors expressing fast-maturing RFP. *Biotechniques* **36**, 436-440, 442.

**Bate, M.** (1990). The embryonic development of larval muscles in *Drosophila*. *Development* **110**, 791-804.

**Baylies, M. K., Bate, M. and Ruiz Gomez, M.** (1998). Myogenesis: a view from Drosophila. *Cell* **93**, 921-927.

**Beckett, K. and Baylies, M. K.** (2006). Parcas, a regulator of non-receptor tyrosine kinase signaling, acts during anterior-posterior patterning and somatic muscle development in Drosophila melanogaster. *Dev. Biol.* **299**, 176-192.

**Beckett, K. and Baylies, M. K.** (2007). 3D analysis of founder cell and fusion competent myoblast arrangements outlines a new model of myoblast fusion. *Dev. Biol.* **309**, 113-115.
**Bogdan, S. and Klambt, C.** (2003). Kette regulates actin dynamics and genetically interacts with Wave and Wasp. *Development* **130**, 4427-4437.
**Bour, B. A., Chakravarti, M., West, J. M. and Abmayr, S. M.** (2000). Drosophila SNS, a member of the immunoglobulin superfamily that is essential for myoblast fusion. *Genes Dev.* **14**, 1498-1511.
**Capovilla, M., Kambris, Z. and Botas, J.** (2001). Direct regulation of the muscle-identity gene apterous by a Hox protein in the somatic mesoderm. *Development* **128**, 1221-1230.
**Carmena, A. and Baylies, M.** (2006). Development of the larval somatic musculature. In *Muscle Development in Drosophila* (ed. H. Sink), pp. 79-89. New York: Landes Bioscience.
**Chen, E. H. and Olson, E. N.** (2001). Antisocial, an intracellular adaptor protein, is required for myoblast fusion in Drosophila. *Dev. Cell* **1**, 705-715.
**Chen, E. H. and Olson, E. N.** (2004). Towards a molecular pathway for myoblast fusion in Drosophila. *Trends Cell Biol.* **14**, 452-460.
**Chen, E. H. and Olson, E. N.** (2005). Unveiling the mechanisms of cell-cell fusion. *Science* **308**, 369-373.
**Chen, E. H., Pryce, B. A., Tzeng, J. A., Gonzalez, G. A. and Olson, E. N.** (2003). Control of myoblast fusion by a guanine nucleotide exchange factor, loner, and its effector ARF6. *Cell* **114**, 751-762.
**Chou, T. B. and Perrimon, N.** (1996). The autosomal FLP-DFS technique for generating germline mosaics in Drosophila melanogaster. *Genetics* **144**, 1673-1679.
**Doberstein, S. K., Fetter, R. D., Mehta, A. Y. and Goodman, C. S.** (1997). Genetic analysis of myoblast fusion: blown fuse is required for progression beyond the prefusion complex. *J. Cell Biol.* **136**, 1249-1261.
**Donaldson, J. G.** (2003). Multiple roles for Arf6: sorting, structuring, and signaling at the plasma membrane. *J. Biol. Chem.* **278**, 41573-41576.
**Duan, H., Skeath, J. B. and Nguyen, H. T.** (2001). *Drosophila* Lame duck, a novel member of the Gli superfamily, acts as a key regulator of myogenesis by controlling fusion-competent myoblast development. *Development* **128**, 4489-4500.
**Dunin-Borkowski, O. M. and Brown, N. H.** (1995). Mammalian CD2 is an effective heterologous marker of the cell surface in Drosophila. *Dev. Biol.* **168**, 689-693.
**Dworak, H. A., Charles, M. A., Pellerano, L. B. and Sink, H.** (2001). Characterization of *Drosophila hibris*, a gene related to human *nephrin*. *Development* **128**, 4265-4276.
**Eden, S., Rohatgi, R., Podtelejnikov, A. V., Mann, M. and Kirschner, M. W.** (2002). Mechanism of regulation of WAVE1-induced actin nucleation by Rac1 and Nck. *Nature* **418**, 790-793.
**Egea, G., Lazaro-Dieguez, F. and Vilella, M.** (2006). Actin dynamics at the Golgi complex in mammalian cells. *Curr. Opin. Cell Biol.* **18**, 168-178.
**Erickson, M. R., Galletta, B. J. and Abmayr, S. M.** (1997). Drosophila myoblast city encodes a conserved protein that is essential for myoblast fusion, dorsal closure, and cytoskeletal organization. *J. Cell Biol.* **138**, 589-603.
**Frasch, M.** (1999). Controls in patterning and diversification of somatic muscles during Drosophila embryogenesis. *Curr. Opin. Genet. Dev.* **9**, 522-529.
**Hakeda-Suzuki, S., Ng, J., Tzu, J., Dietzl, G., Sun, Y., Harms, M., Nardine, T., Luo, L. and Dickson, B. J.** (2002). Rac function and regulation during Drosophila development. *Nature* **416**, 438-442.
**Halfon, M. S., Gisselbrecht, S., Lu, J., Estrada, B., Keshishian, H. and Michelson, A. M.** (2002). New fluorescent protein reporters for use with the Drosophila Gal4 expression system and for vital detection of balancer chromosomes. *Genesis* **34**, 135-138.
**Hasegawa, H., Kiyokawa, E., Tanaka, S., Nagashima, K., Gotoh, N., Shibuya, M., Kurata, T. and Matsuda, M.** (1996). DOCK180, a major CRK-binding protein, alters cell morphology upon translocation to the cell membrane. *Mol. Cell. Biol.* **16**, 1770-1776.
**Horsley, V. and Pavlath, G. K.** (2004). Forming a multinucleated cell: molecules that regulate myoblast fusion. *Cells Tissues Organs* **176**, 67-78.
**Hummel, T., Leifker, K. and Klambt, C.** (2000). The Drosophila HEM-2/NAP1 homolog KETTE controls axonal pathfinding and cytoskeletal organization. *Genes Dev.* **14**, 863-873.
**Ibarra, N., Pollitt, A. and Insall, R. H.** (2005). Regulation of actin assembly by SCAR/WAVE proteins. *Biochem. Soc. Trans.* **33**, 1243-1246.
**Ibarra, N., Blagg, S. L., Vazquez, F. and Insall, R. H.** (2006). Nap1 regulates Dictyostelium cell motility and adhesion through SCAR-dependent and -independent pathways. *Curr. Biol.* **16**, 717-722.
**Kaksonen, M., Toret, C. P. and Drubin, D. G.** (2006). Harnessing actin dynamics for clathrin-mediated endocytosis. *Nat. Rev. Mol. Cell Biol.* **7**, 404-414.
**Kesper, D. A., Stute, C., Buttgereit, D., Kreiskother, N., Vishnu, S., Fischbach, K. F. and Renkawitz-Pohl, R.** (2007). Myoblast fusion in Drosophila melanogaster is mediated through a fusion-restricted myogenic-adhesive structure (FuRMAS). *Dev. Dyn.* **236**, 404-415.
**Kim, S., Shilagardi, K., Zhang, S., Hong, S. N., Sens, K. L., Bo, J., Gonzalez, G. A. and Chen, E. H.** (2007). A critical function for the actin cytoskeleton in targeted exocytosis of prefusion vesicles during myoblast fusion. *Dev. Cell* **12**, 571-586.
**Kiyokawa, E., Hashimoto, Y., Kobayashi, S., Sugimura, H., Kurata, T. and Matsuda, M.** (1998). Activation of Rac1 by a Crk SH3-binding protein, DOCK180. *Genes Dev.* **12**, 3331-3336.
**Kunda, P., Craig, G., Dominguez, V. and Baum, B.** (2003). Abi, Sra1, and Kette control the stability and localization of SCAR/WAVE to regulate the formation of actin-based protrusions. *Curr. Biol.* **13**, 1867-1875.
**Lefevre, G., Jr and Green, M. M.** (1972). Genetic duplication in the white-split interval of the X chromosome in Drosophila melanogaster. *Chromosoma* **36**, 391-412.
**Liu, A. P. and Fletcher, D. A.** (2006). Actin polymerization serves as a membrane domain switch in model lipid bilayers. *Biophys. J.* **91**, 4064-4070.
**Luo, L., Liao, Y. J., Jan, L. Y. and Jan, Y. N.** (1994). Distinct morphogenetic functions of similar small GTPases: Drosophila Drac1 is involved in axonal outgrowth and myoblast fusion. *Genes Dev.* **8**, 1787-1802.
**Machesky, L. M. and Insall, R. H.** (1998). Scar1 and the related Wiskott-Aldrich syndrome protein, WASP, regulate the actin cytoskeleton through the Arp2/3 complex. *Curr. Biol.* **8**, 1347-1356.
**Massarwa, R., Carmon, S., Shilo, B. Z. and Schejter, E. D.** (2007). WIP/WASp-based actin-polymerization machinery is essential for myoblast fusion in Drosophila. *Dev. Cell* **12**, 557-569.
**Menon, S. D. and Chia, W.** (2001). Drosophila rolling pebbles: a multidomain protein required for myoblast fusion that recruits D-Titin in response to the myoblast attractant Dumbfounded. *Dev. Cell* **1**, 691-703.
**Menon, S. D., Osman, Z., Chenchill, K. and Chia, W.** (2005). A positive feedback loop between Dumbfounded and Rolling pebbles leads to myotube enlargement in Drosophila. *J. Cell Biol.* **169**, 909-920.
**Nolan, K. M., Barrett, K., Lu, Y., Hu, K. Q., Vincent, S. and Settleman, J.** (1998). Myoblast city, the Drosophila homolog of DOCK180/CED-5, is required in a Rac signaling pathway utilized for multiple developmental processes. *Genes Dev.* **12**, 3337-3342.
**Nose, A., Isshiki, T. and Takeichi, M.** (1998). Regional specification of muscle progenitors in *Drosophila*: the role of the msh homeobox gene. *Development* **125**, 215-223.
**Patel, K., Christ, B. and Stockdale, F. E.** (2002). Control of muscle size during embryonic, fetal, and adult life. *Results Probl. Cell Differ.* **38**, 163-186.
**Qualmann, B. and Kessels, M. M.** (2002). Endocytosis and the cytoskeleton. *Int. Rev. Cytol.* **220**, 93-144.
**Radhakrishna, H., Al-Awar, O., Khachikian, Z. and Donaldson, J. G.** (1999). ARF6 requirement for Rac ruffling suggests a role for membrane trafficking in cortical actin rearrangements. *J. Cell Sci.* **112**, 855-866.
**Rau, A., Buttgereit, D., Holz, A., Fetter, R., Doberstein, S. K., Paululat, A., Staudt, N., Skeath, J., Michelson, A. M. and Renkawitz-Pohl, R.** (2001). *rolling pebbles* (*rols*) is required in *Drosophila* muscle precursors for recruitment of myoblasts for fusion. *Development* **128**, 5061-5073.
**Rogers, S. L., Wiedemann, U., Stuurman, N. and Vale, R. D.** (2003). Molecular requirements for actin-based lamella formation in *Drosophila* S2 cells. *J. Cell Biol.* **162**, 1079-1088.
**Rorth, P.** (1996). A modular misexpression screen in Drosophila detecting tissue-specific phenotypes. *Proc. Natl. Acad. Sci. USA* **93**, 12418-12422.
**Ruiz-Gomez, M., Coutts, N., Price, A., Taylor, M. V. and Bate, M.** (2000). Drosophila dumbfounded: a myoblast attractant essential for fusion. *Cell* **102**, 189-198.
**Rushton, E., Drysdale, R., Abmayr, S. M., Michelson, A. M. and Bate, M.** (1995). Mutations in a novel gene, *myoblast city*, provide evidence in support of the founder cell hypothesis for *Drosophila* muscle development. *Development* **121**, 1979-1988.
**Schafer, G., Weber, S., Holz, A., Bogdan, S., Schumacher, S., Muller, A., Renkawitz-Pohl, R. and Onel, S. F.** (2007). The Wiskott-Aldrich syndrome protein (WASP) is essential for myoblast fusion in Drosophila. *Dev. Biol.* **304**, 664-674.
**Schroter, R. H., Lier, S., Holz, A., Bogdan, S., Klambt, C., Beck, L. and Renkawitz-Pohl, R.** (2004). *kette* and *blown fuse* interact genetically during the second fusion step of myogenesis in *Drosophila*. *Development* **131**, 4501-4509.
**Schroter, R. H., Buttgereit, D., Beck, L., Holz, A. and Renkawitz-Pohl, R.** (2006). Blown fuse regulates stretching and outgrowth but not myoblast fusion of the circular visceral muscles in Drosophila. *Differentiation* **74**, 608-621.
**Smith, L. G. and Li, R.** (2004). Actin polymerization: riding the wave. *Curr. Biol.* **14**, R109-R111.
**Spradling, A. C., Stern, D., Beaton, A., Rhem, E. J., Laverty, T., Mozden, N., Misra, S. and Rubin, G. M.** (1999). The Berkeley Drosophila Genome Project gene disruption project: single P-element insertions mutating 25% of vital Drosophila genes. *Genetics* **153**, 135-177.
**Stamnes, M.** (2002). Regulating the actin cytoskeleton during vesicular transport. *Curr. Opin. Cell Biol.* **14**, 428-433.
**Steffen, A., Rottner, K., Ehinger, J., Innocenti, M., Scita, G., Wehland, J. and Stradal, T. E.** (2004). Sra-1 and Nap1 link Rac to actin assembly driving lamellipodia formation. *EMBO J.* **23**, 749-759.
**Strunkelnberg, M., Bonengel, B., Moda, L. M., Hertenstein, A., de Couet, H.**

**G., Ramos, R. G. and Fischbach, K. F.** (2001). rst and its paralogue kirre act redundantly during embryonic muscle development in Drosophila. *Development* **128**, 4229-4239.
**Taylor, M. V.** (2003). Muscle differentiation: signalling cell fusion. *Curr. Biol.* **13**, R964-R966.
**Vartiainen, M. K. and Machesky, L. M.** (2004). The WASP-Arp2/3 pathway: genetic insights. *Curr. Opin. Cell Biol.* **16**, 174-181.
**Verkhusha, V. V., Tsukita, S. and Oda, H.** (1999). Actin dynamics in lamellipodia of migrating border cells in the Drosophila ovary revealed by a GFP-actin fusion protein. *FEBS Lett.* **445**, 395-401.
**Wang, X., Willenbring, H., Akkari, Y., Torimaru, Y., Foster, M., Al-Dhalimy, M., Lagasse, E., Finegold, M., Olson, S. and Grompe, M.** (2003). Cell fusion is the principal source of bone-marrow-derived hepatocytes. *Nature* **422**, 897-901.
**Weimann, J. M., Johansson, C. B., Trejo, A. and Blau, H. M.** (2003). Stable reprogrammed heterokaryons form spontaneously in Purkinje neurons after bone marrow transplant. *Nat. Cell Biol.* **5**, 959-966.
**Zallen, J. A., Cohen, Y., Hudson, A. M., Cooley, L., Wieschaus, E. and Schejter, E. D.** (2002). SCAR is a primary regulator of Arp2/3-dependent morphological events in Drosophila. *J. Cell Biol.* **156**, 689-701.
**Zhang, Q., Calafat, J., Janssen, H. and Greenberg, S.** (1999). ARF6 is required for growth factor- and rac-mediated membrane ruffling in macrophages at a stage distal to rac membrane targeting. *Mol. Cell. Biol.* **19**, 8158-8168.
**Zhang, Y., Featherstone, D., Davis, W., Rushton, E. and Broadie, K.** (2000). *Drosophila* D-titin is required for myoblast fusion and skeletal muscle striation. *J. Cell Sci.* **113**, 3103-3115.